Ultrafast polarization switching in $BaTiO_3$ by photoactivation of its ferroelectric and central modes

Fangyuan Gu[1] and Paul Tangney[2]

[1] *Tsung-Dao Lee Institute, Shanghai Jiao Tong University, Pudong, Shanghai 201210, China**
[2] *Department of Physics and Department of Materials, Imperial College London, London SW7 2AZ, UK*

(Dated: January 23, 2024)

We use molecular dynamics simulations with machine-learned atomistic force fields to simulate photoexcitation of $BaTiO_3$ by a femtosecond laser pulse whose photon energy exceeds the optical gap. We demonstrate selective displacive excitation of coherent zone-center ferroelectric mode phonons and of the strongly anharmonic central mode. We show that the direction of **P** can either be reversed by a pulse in hundreds of femtoseconds or, on a longer time scale and when combined with a weak field, switched to any one of its symmetry-equivalent directions.

The most finely-detailed patterns that can be imposed on a crystal's structure quickly, reliably, and reversibly, for the purpose of storing information, are those imposed on ferroic crystals by manipulating their ferroic domains. The fastest way to influence those domains is with ultrashort laser pulses. Many pulse-based mechanisms of manipulating polarization (**P**) domains in ferroelectric (FE) materials have been proposed [1–14], but none of them are ready for widespread use in devices. They tend either to use terahertz (THz)-frequency pulses, which couple strongly and directly to optical phonons [3–6], or to domain walls [7–9, 15, 16]; or they use optical pulses, which excite phonons by impulsive stimulated Raman scattering (ISRS) [17–19]. A disadvantage of THz radiation is that the forces it exerts change directions on phonon time scales. Therefore using it to permanently switch **P** requires pulses to be carefully shaped, polarized and/or coordinated [3, 6, 7, 21, 22]. A disadvantage of ISRS is that it involves high-intensity pulses, which can damage a FE material [3, 17, 20].

$BaTiO_3$ is a widely used and intensively studied FE material, which is often regarded as a prototypical ferroelastoelectric material. In this work we show that above-optical-gap ($>E_g$) photoexcitation with femtosecond (fs) laser pulses could change the direction of **P** in $BaTiO_3$ within hundreds of fs by a deterministic mechanism known as *displacive excitation of coherent phonons* (DECP) [23–29]. Although $>>E_g$ photons produce a lot of heat in pure $BaTiO_3$, there are various ways to mitigate or resolve this problem, such as by doping [29] or using (Sr,Ba)TiO_3 or another similar material whose optical gap is smaller. Furthermore, what makes DECP particularly promising as a **P**-control mechanism is its robustness and versatility: with low intensity pulses, which produce less heat, it can accelerate **P**-switching by other mechanisms and stimuli.

We present the results of atomistic molecular dynamics (MD) simulations which show that $>E_g$ photoexcitation with a fs laser pulse can reverse the direction of **P** within ~ 100 fs, or lower the coercive field strength (E_c) for long enough to switch it with a relatively-weak applied field. It can also induce a temporary displacive transition to the unpolarized cubic $Pm\bar{3}m$ structure of $BaTiO_3$'s paraelectric (PE) phase. This structure would spontaneously polarize again, via a quasi-random process of domain nucleation and growth, when the photoexcited carriers recombined or dispersed. By biasing this process with an applied field or GHz/THz pulses, **P** could be manipulated into any one of its symmetry-equivalent directions.

As in previous works [14, 25, 27–32], we approximate the absorption of a fs $>E_g$ pulse as an instantaneous change to the state of the electrons, which takes them out of thermal equilibrium with the lattice, and creates two separate thermalized populations of carriers: conduction band electrons and valence band holes. These carriers' densities (x) are equal, initially, and remain approximately constant for several ps [14, 25, 27–29, 31, 32].

Although we neglect the ~ 100's of fs [33–36] taken for the populations of electrons and holes to thermalize, the DECP mechanism by which a fs $>E_g$ pulse interacts with **P** does not require this thermalization, or wait for it to happen. It begins as soon as electrons vacate bonding states and occupy anti-bonding states, because it is driven by the forces on the crystal's sublattices caused by this change of the electron density. Qualitatively, and semi-quantitatively, these forces are determined by x and by the characters of the upper valence band states ($\approx$ O-2p admixed with Ti-3d) and lower conduction band states ($\approx$ Ti-3d admixed with O-2p). They are relatively insensitive to how holes and electrons, respectively, are distributed among these states [29].

DECP occurs when a high density of photoexcited carriers is created by a fs laser pulse in a crystal that possesses A_1 phonon modes. A_1 phonons are excited by $>E_g$ photoexcitation because the meaning of a mode having A_1 symmetry is that both its equilibrium and average mode coordinates are not constrained by symmetry. Therefore they are changed, to some degree, by any stimulus. When a laser pulse changes a crystal's A_1 mode coordinates suddenly, by redistributing electron

* fangyuan.gu@sjtu.edu.cn

density and weakening bonds, the crystal's sublattices suddenly have the wrong relative displacements. Therefore they move along the A_1 eigenvectors towards the new A_1 coordinates, which they overshoot and oscillate about [24, 25, 29]. This oscillation is the displacively-excited coherent A_1 phonon.

$BaTiO_3$ has three FE phases, which all possess A_1 modes and have almost identical electronic structures. Each FE phase only differs from the $Pm\bar{3}m$ structure by tiny symmetry-breaking relative displacements of its sublattices along its A_1 eigenvectors, which lower the potential energy by $\Delta U \equiv U_{Pm\bar{3}m} - U_{FE} > 0$, and create a $\mathbf{P}$ field [29]. By far the largest contributions to both $\mathbf{P}$ and ΔU come from the *polar distortion* of $Pm\bar{3}m$ along the eigenvector of the FE phase's A_1 *ferroelectric mode* (FM), which is a counter-motion of the Ti and O sublattices along an axis parallel to $\mathbf{P}$. The polar disortion makes the Ti-O Coulombic attraction more negative by shortening the Ti-O bond length, and the displacements along the other A_1 eigenvectors help to accommodate it [29].

We simulated ultrafast $>E_g$ photoexcitation of $BaTiO_3$'s R3m FE phase, which has three optical A_1 modes; namely, the FM, the *Axe mode* (AM) [37], and the *Last mode* (LM) [38]. Both the FM and its counterpart in $Pm\bar{3}m$, which does not have A_1 symmetry, are often referred to as the *soft mode* or the *Slater mode* (SM) [39]. We refer to it as the FM when its A_1 symmetry is relevant and as the SM otherwise. Ultrafast $>E_g$ photoexcitation induces motion along every A_1 eigenvector to some degree, but it *selectively* excites motion along the FM eigenvector in the sense that the AM and LM are excited to much lesser degrees. Before demonstrating this selectivity, we briefly explain it. We discuss it in greater detail in Ref. 29.

Roughly-speaking, the SM of a given phase can be viewed as an oscillation of $\Delta_{Ti\text{-}O} \equiv d^{Pm\bar{3}m}_{Ti\text{-}O} - d_{Ti\text{-}O} \geq 0$, where $d_{Ti\text{-}O}$ and $d^{Pm\bar{3}m}_{Ti\text{-}O}$ are the Ti-O nearest-neighbour distances in the given phase and in $Pm\bar{3}m$, respectively. We choose the origin for the FM mode coordinate, Q_{FM}, to be where the polar distortion vanishes, i.e., in the $Pm\bar{3}m$ phase. Therefore the thermodynamic averages of Q_{FM}, $\Delta_{Ti\text{-}O}$, $\mathbf{P}$, and the contribution, $\mathbf{P}_{FM}$, of the polar distortion to $\mathbf{P}$, approximately satisfy $\bar{\mathbf{P}}(T,x) \approx \bar{\mathbf{P}}_{FM}(T,x) \propto \bar{Q}_{FM}(T,x) \propto \bar{\Delta}_{Ti\text{-}O}(T,x)$. Photoexcited carriers weaken the Ti-O attraction by screening it and by reducing the magnitudes of Ti and O ions' charges [29]. They reduce charges because promoting electrons from predominantly O-2p bonding states to predominantly Ti-3d anti-bonding states moves some electron density from O to Ti. Therefore DECP excites the FM strongly because $Q_{FM} \propto \Delta_{Ti\text{-}O}$ is highly sensitive to x. However, the AM and LM do not depend linearly on $\Delta_{Ti\text{-}O}$ and there is no obvious reason why DECP would excite them strongly.

We performed MD simulations with dipole-polarizable and variable-charge machine-learned atomistic force fields, as described in the Supplementary Material and Ref. 40. We parameterized three force fields: To model interactions before absorption of a laser pulse we fit the parameters to density functional theory (DFT) calculations of thermally-disordered crystals with electrons in their ground state ($x = 0$). To model interactions after pulse absorption, we parameterized force fields for $x = 0.05$ electrons per $BaTiO_3$ formula unit (e^-/ f.u.) and $x = 0.12$ e^-/ f.u. by fitting the parameters to constrained-DFT calculations, as described in Refs. 25, 28, and 29. We used a $12 \times 12 \times 12$ supercell (8640 atoms), under periodic boundary conditions, and performed long MD simulations with the $x = 0$ potential to equilibrate, before modelling fs $>E_g$ pulse absorption by switching abruptly to one of the photoexcited potentials. We calculated the $\mathbf{P}$ autocorrelation function, $\langle \mathbf{P}(t_0)\mathbf{P}(t_0+t)\rangle_{t_0}$, from the first 10 ps after photoexcitation and Fourier transformed it to calculate the infrared (IR) absorption spectrum.

Both ΔU and the FE to PE transition temperature, T_C, are highly sensitive to strain and are lowered by compression [41]. Therefore, when force fields or DFT overestimate the density, it is common to perform calculations at the experimental density or under negative pressure [42, 43]. We found $T_C \approx 150$ K, $T_C \approx 100$ K, and $T_C \approx 50$ K for our $x = 0$, $x = 0.05$ e^-/ f.u., and $x = 0.12$ e^-/ f.u. force fields, respectively. However we chose not to apply negative pressure because working at a low T allowed us to observe the DECP mechanism with less thermal noise, and to calculate spectra with signal-to-noise ratios closer to those that would be obtained with simulation cells comparable in size to the photoexcited regions in pump-probe experiments.

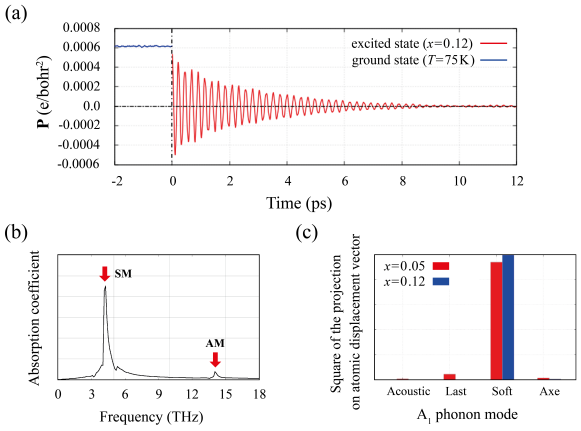

FIG. 1. (a) Polarization, $\mathbf{P}$, as a function of time (t), with $>E_g$ photoexcitation to a carrier density of $x = 0.12$ e^-/ f.u. occurring at $t = 0$; (b) The IR absorption spectrum immediately after photoexcitation; (c) Squared projections of the $\sqrt{\text{mass}}$-scaled atomic displacement vectors onto the three zone-center A_1 optical phonon eigenvectors. The sums of the squared projections are one.

Figure 1(a) is a plot of $\mathbf{P}$ as function of time (t) in MD simulations of photoexcitation to a carrier density of $x = 0.12$ e^-/ f.u. at $T = 75$ K. At

$t = 0$, photoexcitation changes the value of $\mathbf{P}$ at thermal equilibrium from $\bar{\mathbf{P}}(75\text{ K}, 0) \approx 6 \times 10^{-4}\ e^-/\text{bohr}$ to $\bar{\mathbf{P}}(75\text{ K}, 0.12\ e^-/\text{f.u.}) = 0$. The latter vanishes because Pm$\bar{3}$m is the thermodynamically stable phase at $(T, x) = (75\text{ K}, 0.12\ e^-/\text{f.u.})$ with our force field. Therefore the fs pulse causes $\bar{\mathbf{P}}$ to vanish suddenly as a consequence of $\bar{Q}_{\text{FM}}$ and $\bar{\Delta}_{\text{Ti-O}}$ vanishing suddenly. The change of $\bar{Q}_{\text{FM}}$ excites a large amplitude SM phonon by displacively exciting motion along the FM eigenvector. This manifests in Fig. 1 as a damped oscillation of $\mathbf{P}$ about $\mathbf{P} = 0$, with an initial amplitude of $\left|\bar{\mathbf{P}}(75\text{ K}, 0)\right|$. Figure 1(b) is the IR absorption spectrum calculated immediately after photoexcitation, and Fig. 1(c) shows the decomposition, into components along the A_1 eigenvectors, of the lattice's displacement from its new equilibrium immediately after photoexcitation. These plots demonstrate that DECP selectively excites the SM.

To better understand what happens when a fs $>E_g$ pulse is absorbed, it is useful to regard the FM as an oscillation of $\mathbf{P}$. If $\mathbf{p}_\alpha$ denotes the dipole moment of the α^{th} primitive cell of the crystal divided by its volume, then $\mathbf{P}$ is the average of $\mathbf{p}_\alpha$ over all cells α; and $\bar{\mathbf{P}}(T, x)$ is the value shared by $\mathbf{P}$ and the time-average of each $\mathbf{p}_\alpha(t)$ at thermal equilibrium. Therefore a displacively-excited FM phonon can be viewed as a collective motion of the set $\{\mathbf{p}_\alpha\}$ of all $\mathbf{p}$'s, which is caused by a sudden change of $\bar{\mathbf{P}}$ from $\bar{\mathbf{P}}(T, 0)$ to $\bar{\mathbf{P}}(T, x)$, and which has an initial amplitude of $\Delta\bar{\mathbf{P}}(T, x) \equiv \left|\bar{\mathbf{P}}(T, 0) - \bar{\mathbf{P}}(T, x)\right|$. The motion is collective in the statistical sense that the *average* time derivative of the $\mathbf{p}$'s is finite, and remains finite until the crystal reaches a new thermal equilibrium in which the time averages of the $\mathbf{p}$'s are all equal to $\bar{\mathbf{P}}(T, x)$.

Now consider a simple model of the crystal in which $\mathbf{p}_\alpha$ completely specifies the structure of the α^{th} cell, and $\bar{\mathbf{P}} = \bar{\mathbf{P}}_{\text{FM}}$. Although it is simplistic and wrong to describe the interactions between neighboring cells as dipole-dipole couplings, we assume that the strain of each cell is correlated strongly enough with its dipole moment to allow interactions between cells, including the coupling between their strains, to be approximated by a function of their dipole moments. Therefore, let $u_\alpha(\mathbf{p}_\alpha; T, x, t)$ denote the potential energy *of the entire crystal* as a function of $\mathbf{p}_\alpha$, when all other $\mathbf{p}$'s are fixed at their values at time t. Let $\bar{u}(\mathbf{p}; T, x)$ denote the average of u_α, over all α or over time, at thermal equilibrium; and let $U(\mathbf{P}; T, x)$ denote the thermodynamic average of the potential energy over all microstates of the crystal for which $\mathbf{P}_{\text{FM}} = \mathbf{P}$.

Each u_α is time dependent because it is highly sensitive to the structures and strains of surrounding cells [43]. Instantaneously, it is not symmetric about $\mathbf{p}_\alpha = 0$, and it may be a single well or an asymmetric double well, with the (deeper) minimum continuously moving as the $\mathbf{p}$'s of surrounding cells change [43]. However $U(\mathbf{P}; T, x)$ and $\bar{u}(\mathbf{p}; T, x)$ are independent of t because they are thermodynamic averages. Figure 2 shows schematic cross sections of them, along the axis passing through $\bar{\mathbf{P}}_{\text{FM}}$ and $-\bar{\mathbf{P}}_{\text{FM}}$, as both T and x are varied. When

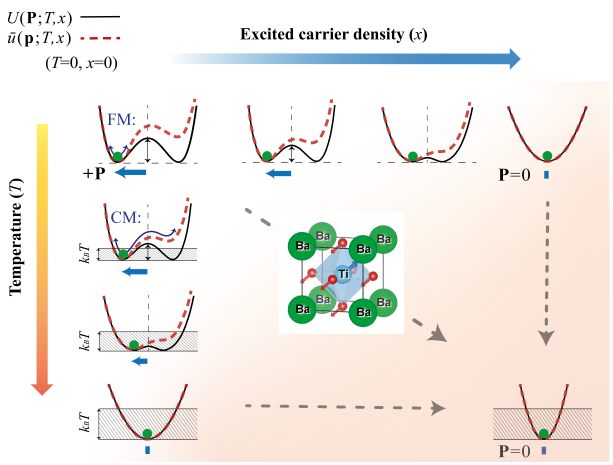

FIG. 2. Schematic illustrating the average potential energy, U and $\bar{u}$, as a function of $\mathbf{P}$ and $\mathbf{p}$, respectively, at $T = 0$ in the electronic ground state and at several temperatures (T) and photoexcited carrier densities (x). The $BaTiO_3$ crystal structure in the center demonstrates the FM eigenvector of the R3m phase.

$(T, x) \approx (0, 0)$, U is a symmetric double well, with the wells at $\mathbf{P} = \pm\bar{\mathbf{P}}_{\text{FM}}(T, x)$ corresponding to symmetry-equivalent R3m structures. The energy barrier separating them is at $\mathbf{P} = 0$, which corresponds to the Pm$\bar{3}$m structure within this simple model, and its height is $\Delta U(T, x) \equiv U(0; T, x) - U(\bar{\mathbf{P}}_{\text{FM}}(T, x); T, x)$.

The zone-center FM is a coherent collective oscillation of the $\mathbf{p}$'s about $\mathbf{p} = \bar{\mathbf{P}}_{\text{FM}}$. Both experimentally [44, 45], and in our $x = 0$ simulations (Fig. 3), increasing T causes the FM's IR absorption peak to soften and broaden, and a very broad peak, known as the *central mode* (CM), to emerge in the frequency range $0 - 3$ THz. The CM is not one of the crystal's normal modes, and it does not exist in the $T \to 0$ limit. It gradually becomes active as T increases and the directions of the $\mathbf{p}$'s become disordered.

It is common to view the dynamics of each $\mathbf{p}_\alpha$ as motion on a potential energy surface with eight minima [29, 46–48]. At each minimum, $\mathbf{p}_\alpha$ is parallel to one of the four body diagonals of the cubic cell shown in Fig. 2, and is directed towards a different one of the eight corner Ba atoms [49–51]. The CM is often thought of as a collective hopping motion of the $\mathbf{p}$'s between two or more of these eight minima. However, Fallon's calculations of u_α for various structures of surrounding cells (Ref. 43, Sec. 7.4) suggest that it may be more realistic to view $\mathbf{p}_\alpha$ as moving on a continuously-changing surface with only one minimum. Therefore, instead of $\mathbf{p}_\alpha$ hopping between eight ever-present minima of a relatively-passive potential energy surface, it might simply follow a single minimum around as it is moved by the rapidly-changing $\mathbf{p}$'s of surrounding cells.

Regardless of how active a role the time dependence of u_α plays, the CM peak is the spectral signature of the relatively slow and anharmonic large-amplitude 'rattling'

of the $\mathbf{p}$'s between multiple directions, which emerges as they gain enough thermal energy to change direction. At low T, when most $\mathbf{p}$'s are aligned, $\mathbf{p}_\alpha$ spends most of its time near the $\mathbf{p}_\alpha \parallel \mathbf{P}$ site. As T increases it spends an increasing fraction of its time at the other seven sites. Therefore the directional disorder of the $\mathbf{p}$'s reduces $\left|\bar{\mathbf{P}}\right|$ and $\left|\bar{\mathbf{P}}_{\rm FM}\right|$ and, if our revision of the eight-site model is realistic, it makes $\bar{u}$ more symmetric because the minimum of u_α spends more of its time at the $\mathbf{p}_\alpha \parallel (-\mathbf{P})$ site. Disorder also reduces ΔU because the potential energy is lower when each $\mathbf{p}$ is parallel to its neighbours. Reducing $\Delta U/(k_B T)$ increases the proportion of time for which the direction of each $\mathbf{p}$ differs significantly from that of $\mathbf{P}$, and reduces the fraction of the $\mathbf{p}$'s that, at any given time, are participating in the FM, i.e., performing small synchronized oscillations about energy minima at their $\mathbf{p} \parallel \mathbf{P}$ sites. Therefore, when the CM becomes active it amplifies itself by generating disorder that makes it easier for the $\mathbf{p}$'s to change direction.

The FM IR absorption peak shrinks as the CM peak grows with increasing T because, as more $\mathbf{p}$'s contribute to the CM, fewer are available to participate in it. It also softens and broadens because reducing ΔU makes the wells in U shallower, which reduces their curvatures and makes them less harmonic. As T increases even further, the $\mathbf{p}$'s becomes so disordered that ΔU vanishes and U becomes a single well with a minimum at $\mathbf{P} = 0$. At the lowest values of T for which Pm$\bar{3}$m is stable, U is approximately quartic (i.e., flat-bottomed; see Fig. 2), meaning that a sufficiently-small polar distortion neither raises nor lowers U. When T is larger, U is quadratic near its minimum and its curvature increases as T increases [29].

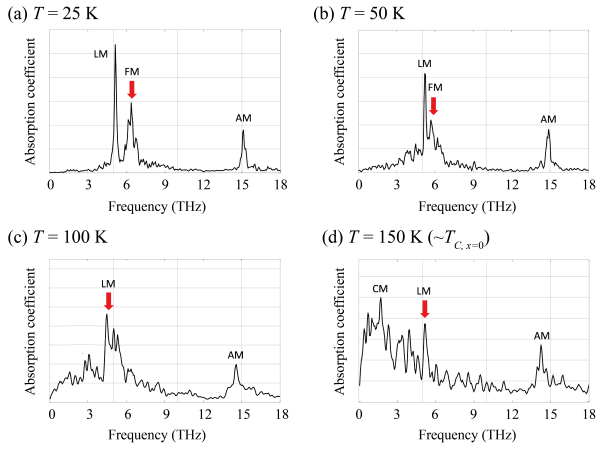

FIG. 3. Infrared absorption spectra in the electronic ground state.

The effects on $\bar{u}$ and U of increasing x are similar to the effects of increasing T: by weakening the Ti-O attraction, photoexcited carriers reduce both ΔU and the magnitude of the polar distortion [29]. Therefore increasing x reduces $\bar{\mathbf{P}}_{\rm FM}$ by moving the two minima of

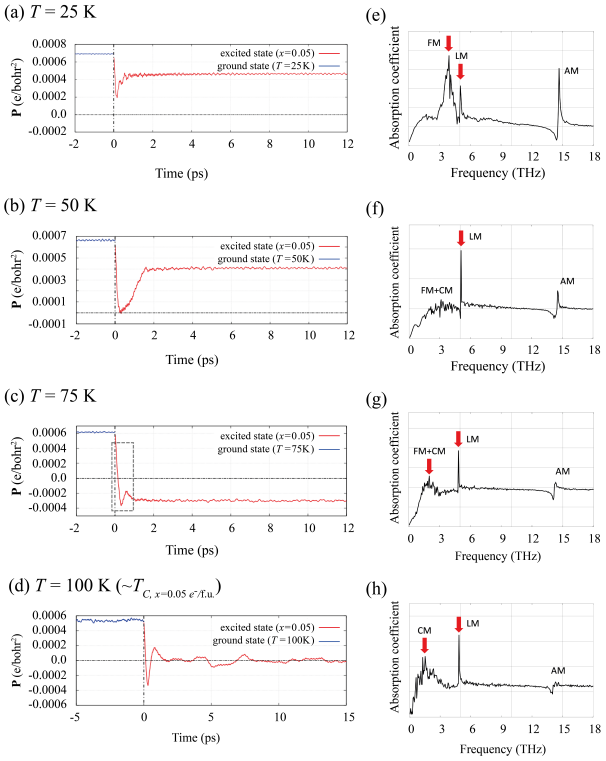

FIG. 4. (a)-(d): $\mathbf{P}$ as a function of time in NPH simulations of ultrafast photoexcitation to a carrier density of of $x = 0.05\ e^-/\text{f.u.}$ at four temperatures. (e)-(h): IR absorption spectra at the same four temperatures immediately after the simulated pulse absorption at $t = 0$.

U closer together and, by making the two energy wells shallower [29], it lowers the FM frequency, makes it less harmonic, and makes the CM more active. Therefore it decreases the proportion of time for which each $\mathbf{p}$ is approximately parallel to $\mathbf{P}$.

There is no CM peak in Fig. 1(b) because, at $(T, x) = (75\ \text{K}, 0.12\ e^-/\text{f.u.})$, the combined effects of x and T make U a single approximately-quadratic well. Instead of the $\mathbf{p}$'s rattling between different directions with very large amplitudes, as they would at lower values of x or T, their collective motion is a superposition of the Pm$\bar{3}$m phase's three degenerate SMs. When x is large or $T - T_C$ is large and positive, each zone-center SM of Pm$\bar{3}$m is an oscillation of one of three mutually-orthogonal components of $\mathbf{P}$ about the approximately-quadratic minimum of a function identical to $U(\mathbf{P}; T, x)$. When x and/or T are either very large or very small, the CM is not active, the minima of U and $\bar{u}$ have relatively-high curvatures, and thermal fluctuations of the $\mathbf{p}$'s are much smaller than when the CM is active.

Figures 4(a)-(d) are plots of $\mathbf{P}(t)$ in simulations of photoexcitation to a much smaller carrier density ($x = 0.05\ e^-/\text{f.u.}$) than in the simulations reported in Fig. 1. R3m is stable at $(T, x) = (75\ \text{K}, 0.05\ e^-/\text{f.u.})$, but

$Pm\bar{3}m$ is stable at $(T, x) = (100\text{ K}, 0.05\ e^-/\text{f.u.})$. The IR spectra in Figs. 4(e)-(h) show the emergence of the CM as T increases, and that the FM has softened before its peak disappears. They also show that, at $T = 100$ K, the CM still has a substantial peak. This implies that the oscillation of $\mathbf{P}$ about $\mathbf{P} = 0$ in Fig. 4(d) is not simply a superposition of small-amplitude harmonic SMs. It implies that the average magnitude of the $\mathbf{p}$'s is large, that the $\mathbf{p}$'s are disordered, that each $\mathbf{p}$ is rattling between multiple directions with a large amplitude, and that U and $\bar{u}$ are either flat, or shallow double wells. This explains why the oscillations about $\mathbf{P} = 0$ in Fig. 4 (d) are so much less harmonic than those in Fig. 1 (a), and why, when $T \leq 75$ K, the damping of the displacively-excited motion along the FM eigenvector is strong enough for $\mathbf{P}$ to stabilize at $\mathbf{P} \approx \bar{\mathbf{P}}(T, 0.05\ e^-/\text{f.u.})$ almost immediately.

The damping of the collective component of the motion of the $\mathbf{p}$'s can be viewed as their motions falling out of synchronicity. It is a crucial ingredient in the pulse-induced $\mathbf{P}$-reversal mechanism that we propose, and which Fig. 4(c) demonstrates. Without it, $\mathbf{P}$ would return to its original direction almost as quickly as it reversed. In Fig. 4(c), $\mathbf{P}$ reverses in less than half a FM period and remains reversed. This demonstrates that, when T is low enough that the FE phase is stable, there exists a pulse fluence for which $\mathbf{P}$ is deterministically and permanently reversed within 100's of fs of pulse absorption.

Pulse-induced $\mathbf{P}$-reversal is permanent, but the reductions of E_c and $\left|\bar{\mathbf{P}}\right|$, and the photoinduced stability of $Pm\bar{3}m$ (Fig. 1(a) and Fig. 4(d)), only last until x is reduced by electron-hole recombination and/or diffusion. During this time, which might be as short as tens of ps or as long as many nanoseconds [33], the ultimate direction of $\mathbf{P}$ could be determined by a weak bias, such as an applied field, or by a different pulse-induced mechanism [6, 13, 52, 53].

In summary, we have shown that fs $>E_g$ pulses would selectively excite motion along $BaTiO_3$'s A_1 FM eigenvector. For a T-dependent range of pulse fluences, this motion would reverse $\mathbf{P}$ within 100's of fs without subsequently returning it to its original direction. Higher pulse fluences would induce a transient transition to the PE phase. Therefore, a slower method of manipulating $\mathbf{P}$, but one capable of placing it into any of its symmetry-equivalent directions, would be to bias the process by which the transient PE phase spontaneously repolarizes when electrons return to their ground state. Our simulations also demonstrate that much could be learned about $BaTiO_3$ and related materials from pump-probe experiments that selectively excite the SM by DECP.

ACKNOWLEDGMENTS

We acknowledge helpful discussions with Éamonn Murray, Wei Ku, Wei Wang, Chi-Ming Yim, Zefang Lv, Jie Chen and financial support from the International Postdoctoral Exchange Fellowship Program (YJ20210137) by the Office of China Postdoc Council (OCPC).

[1] S. Fahy and R. Merlin, Phys. Rev. Lett. **73**, 1122 (1994).
[2] M. W. Wefers, H. Kawashima, and K. A. Nelson, J. Phys. Chem. Sol. **57**, 1425 (1996).
[3] T. Qi, Y.-H. Shin, K.-L. Yeh, K. A. Nelson, and A. M. Rappe, Phys. Rev. Lett. **102**, 247603 (2009).
[4] A. Subedi, Phys. Rev. B **92**, 214303 (2015).
[5] F. Chen, Y. Zhu, S. Liu, Y. Qi, H. Y. Hwang, N. C. Brandt, J. Lu, F. Quirin, H. Enquist, P. Zalden, T. Hu, J. Goodfellow, M.-J. Sher, M. C. Hoffmann, D. Zhu, H. Lemke, J. Glownia, M. Chollet, A. R. Damodaran, J. Park, Z. Cai, I. W. Jung, M. J. Highland, D. A. Walko, J. W. Freeland, P. G. Evans, A. Vailionis, J. Larsson, K. A. Nelson, A. M. Rappe, K. Sokolowski-Tinten, L. W. Martin, H. Wen, and A. M. Lindenberg, Phys. Rev. B **94**, 180104 (2016).
[6] R. Mankowsky, A. von Hoegen, M. Först, and A. Cavalleri, Phys. Rev. Lett. **118**, 197601 (2017).
[7] H. Akamatsu, Y. Yuan, V. A. Stoica, G. Stone, T. Yang, Z. Hong, S. Lei, Y. Zhu, R. C. Haislmaier, J. W. Freeland, L. Chen, H. Wen, and V. Gopalan, Phys. Rev. Lett. **120**, 096101 (2018).
[8] F. Rubio-Marcos, D. A. Ochoa, A. Del Campo, M. A. Garcia, G. R. Castro, J. F. Fernandez, and J. E. Garcia, Nat. Phot. **12**, 29 (2018).
[9] T. Li, A. Lipatov, H. Lu, H. Lee, J.-W. Lee, E. Torun, L. Wirtz, C.-B. Eom, J. Iniguez, A. Sinitskii, and A. Gruverman, Nat. Comm. **9** (2018).
[10] V. I. Yukalov and E. P. Yukalova, Phys. Rev. Res. **1**, 033136 (2019).
[11] A. Kimel, A. Kalashnikova, A. Pogrebna, and A. Zvezdin, Physics Reports **852**, 1 (2020), fundamentals and perspectives of ultrafast photoferroic recording.
[12] A. Bagri, A. Jana, G. Panchal, D. M. Phase, and R. J. Choudhary, ACS Applied Electronic Materials **4**, 4438 (2022).
[13] P. Chen, C. Paillard, H. J. Zhao, J. Iniguez, and L. Bellaiche, Nat. Comm. **13**, 2566 (2022).
[14] L. Gao, C. Paillard, and L. Bellaiche, Phys. Rev. B **107**, 104109 (2023).
[15] F. Rubio-Marcos, A. Del Campo, P. Marchet, and J. F. Fernández, Nat. Comm. **6**, 6594 (2015).
[16] D. Paez-Margarit, F. Rubio-Marcos, D. A. Ochoa, A. Del Campo, J. F. Fernandez, and J. E. Garcia, ACS Appl. Mater. Interfaces **10**, 21804 (2018).
[17] C. J. Brennan and K. A. Nelson, J. Chem. Phys. **107**, 9691 (1997).
[18] A. Cavalleri, S. Wall, C. Simpson, E. Statz, D. W. Ward, K. A. Nelson, M. Rini, and R. W. Schoenlein, Nature **442**, 664 (2006).
[19] K. Istomin, V. Kotaidis, A. Plech, and

Q. Kong, App. Phys. Lett. **90**, 022905 (2007), https://pubs.aip.org/aip/apl/article-pdf/doi/10.1063/1.2430773/14026049/022905_1_online.pdf.
[20] G. P. Wiederrecht, T. P. Dougherty, L. Dhar, K. A. Nelson, A. M. Weiner, and D. E. Leaird, Ferroelectrics **144**, 1 (1993), https://doi.org/10.1080/00150199308008620.
[21] D. S. Rana, I. Kawayama, K. Mavani, K. Takahashi, H. Murakami, and M. Tonouchi, Adv. Mater. **21**, 2881 (2009).
[22] F. Chen, Y. Zhu, S. Liu, Y. Qi, H. Y. Hwang, N. C. Brandt, J. Lu, F. Quirin, H. Enquist, P. Zalden, T. Hu, J. Goodfellow, M.-J. Sher, M. C. Hoffmann, D. Zhu, H. Lemke, J. Glownia, M. Chollet, A. R. Damodaran, J. Park, Z. Cai, I. W. Jung, M. J. Highland, D. A. Walko, J. W. Freeland, P. G. Evans, A. Vailionis, J. Larsson, K. A. Nelson, A. M. Rappe, K. Sokolowski-Tinten, L. W. Martin, H. Wen, and A. M. Lindenberg, Phys. Rev. B **94**, 180104 (2016).
[23] H. J. Zeiger, J. Vidal, T. K. Cheng, E. P. Ippen, G. Dresselhaus, and M. S. Dresselhaus, Phys. Rev. B **45**, 768 (1992).
[24] S. Hunsche, K. Wienecke, T. Dekorsy, and H. Kurz, Phys. Rev. Lett. **75**, 1815 (1995).
[25] P. Tangney and S. Fahy, Phys. Rev. Lett. **82**, 4340 (1999).
[26] M. Bargheer, N. Zhavoronkov, Y. Gritsai, J. Woo, D. Kim, M. Wörner, and T. Elsässer, Science **306**, 1771 (2004).
[27] E. D. Murray, D. M. Fritz, J. K. Wahlstrand, S. Fahy, and D. A. Reis, Phys. Rev. B **72**, 060301 (2005).
[28] P. Tangney and S. Fahy, Phys. Rev. B **65**, 054302 (2002).
[29] F. Gu, E. Murray, and P. Tangney, Phys. Rev. Mater. **5**, 034414 (2021).
[30] E. S. Zijlstra, L. L. Tatarinova, and M. E. Garcia, Phys. Rev. B **74**, 220301 (2006).
[31] E. D. Murray, S. Fahy, D. Prendergast, T. Ogitsu, D. M. Fritz, and D. A. Reis, Phys. Rev. B **75**, 184301 (2007).
[32] D. M. Fritz, D. A. Reis, B. Adams, R. A. Akre, J. Arthur, C. Blome, P. H. Bucksbaum, A. L. Cavalieri, S. Engemann, S. Fahy, R. W. Falcone, P. H. Fuoss, K. J. Gaffney, M. J. George, J. Hajdu, M. P. Hertlein, P. B. Hillyard, M. H.-v. Hoegen, M. Kammler, J. Kaspar, R. Kienberger, P. Krejcik, S. H. Lee, A. M. Lindenberg, B. McFarland, D. Meyer, T. Montagne, E. D. Murray, A. J. Nelson, M. Nicoul, R. Pahl, J. Rudati, H. Schlarb, D. P. Siddons, K. Sokolowski-Tinten, T. Tschentscher, D. von der Linde, and J. B. Hastings, Science **315**, 633 (2007).
[33] S. K. Sundaram and E. Mazur, Nat. Mater. **1**, 217 (2002).
[34] E. Gamaly, Phys. Rep. **508**, 91 (2011).
[35] J. Shah, *Ultrafast Spectroscopy of Semiconductors and Semiconductor Nanostructures*, Springer Series in Solid-State Sciences (Springer Berlin Heidelberg, 2013).
[36] K. C. Phillips, H. H. Gandhi, E. Mazur, and S. K. Sundaram, Adv. Opt. Photon. **7**, 684 (2015).
[37] J. D. Axe, Phys. Rev. **157**, 429 (1967).
[38] J. T. Last, Phys. Rev. **105**, 1740 (1957).
[39] J. C. Slater, Phys. Rev. **78**, 748 (1950).
[40] V. Nemytov, *Towards an accurate and transferable charge transfer model in polarisable interatomic potentials*, Ph.D. thesis, Imperial College London (2019).
[41] V. M. Goldschmidt, Naturewissenschaften **14**, 477 (1926).
[42] W. Zhong, D. Vanderbilt, and K. M. Rabe, Phys. Rev. Lett. **73**, 1861 (1994).
[43] J. Fallon, *Multiscale theory and simulation of barium titanate*, Ph.D. thesis, Imperial College London (2014).
[44] J. Hlinka, T. Ostapchuk, D. Nuzhnyy, J. Petzelt, P. Kuzel, C. Kadlec, P. Vanek, I. Ponomareva, and L. Bellaiche, Phys. Rev. Lett. **101**, 167402 (2008).
[45] J. Weerasinghe, L. Bellaiche, T. Ostapchuk, P. Kužel, C. Kadlec, S. Lisenkov, I. Ponomareva, and J. Hlinka, MRS Commun. **3**, 41–45 (2013).
[46] R. Pirc and R. Blinc, Phys. Rev. B **70**, 134107 (2004).
[47] M. S. Senn, D. A. Keen, T. C. A. Lucas, J. A. Hriljac, and A. L. Goodwin, Phys. Rev. Lett. **116**, 207602 (2016).
[48] L. Gigli, M. Veit, M. Kotiuga, G. Pizzi, N. Marzari, and M. Ceriotti, npj Comput. Mater, **8**, 209 (2022).
[49] I. B. Bersuker, Phys. Lett. **20**, 589 (1966).
[50] R. Comes, M. Lambert, and A. Guinier, Solid State Commun. **6**, 715 (1968).
[51] A. S. Chaves, F. C. S. Barreto, R. A. Nogueira, and B. Zẽks, Phys. Rev. B **13**, 207 (1976).
[52] A. Subedi, Phys. Rev. B **92**, 214303 (2015).
[53] P. Gayathri, M. J. Swamynathan, M. Shaikh, A. Ghosh, and S. Ghosh, Chemistry of Materials **35**, 6612 (2023).